Optics Communications 501 (2021) 127325

Contents lists available at ScienceDirect

Optics Communications

journal homepage: www.elsevier.com/locate/optcom

Optical multimode interference couplers of Ti:$LiNbO_3$ waveguides and electrical tuning of power splitting ratio

Anna Hirai [a], Yuichi Matsumoto [a], Takanori Sato [b], Tadashi Kawai [a], Akira Enokihara [a,*], Shinya Nakajima [c], Naokatsu Yamamoto [c]

[a] Graduate School of Engineering, University of Hyogo, Himeji-shi, Hyogo, 671-2280, Japan
[b] Graduate School of Information Science and Technology, Hokkaido University, Sapporo-shi, Hokkaido, 060-0814, Japan
[c] National Institute of Information and Communications Technology, Koganei-shi, Tokyo, 184-8795, Japan

ARTICLE INFO

Keywords:
Multimode interference (MMI)
Optical coupler
Titanium-diffused $LiNbO_3$ waveguide
Tuning
Power splitting ratio

ABSTRACT

We analyzed the optical properties of optical couplers based on multimode interference (MMI) in titanium-diffused $LiNbO_3$ (Ti:LN) waveguides using the beam propagation method (BPM) with refractive index distributions by Ti diffusion. From these results, we designed and fabricated 2 × 2 MMI couplers operating at 1.55 μm wavelength using Ti:LN waveguides. An optical power splitting ratio of 0.53:0.47 (0.52 dB power deviation from equal split) and an insertion loss of less than 1.5 dB were observed with a coupler consisting of an MMI waveguide 50 μm wide and 2.12 mm long. Electrical tuning of the power splitting ratio by the electro-optic effect of $LiNbO_3$ was also considered. The electrodes were formed directly on the MMI waveguide section of the coupler and the power splitting ratios were controlled almost in proportion to the voltage applied to the electrode and a deviation of about 1 dB (0.56:0.44) of the power splitting ratio from an equal split could be adjusted to zero by applying a voltage of −6.1 V.

1. Introduction

Optical waveguide devices based on multimode interference (MMI) are key elements in various optical integrated circuits [1]. Novel properties of optical couplers not exhibited by conventional devices consisting of single-mode optical waveguides are expected to be achieved in designs with MMI waveguides. Multiport optical couplers, such as optical 90-degree hybrids, are typically used in IQ demodulation in optical fiber communication [2]. Arrayed waveguide gratings have been applied as key components in wavelength division multiplexers [3]. MMI multiport couplers have also been considered for other applications [4,5].

MMI optical devices are fabricated with Si or SiO_2 materials in many cases [6,7]. High dimensional accuracy can be easily obtained using Si microfabrication processes, and integration of optical components with Si electronic circuits is also expected. Therefore Si-based optical waveguide materials have been preferably used for MMI devices.

$LiNbO_3$ as an electro-optic (EO) material has been generally used as a substrate for high-speed optical modulators. Low loss optical waveguides can be easily formed by the thermal diffusion of titanium in $LiNbO_3$. Electrical tuning of the device properties can also be achieved by using the EO effect. If MMI based circuit elements are produced using titanium-diffused $LiNbO_3$ (Ti:LN) waveguides, EO devices with novel features will be achieved by integrating the MMI circuit elements with the optical circuits in the EO devices. As a simple example, we consider the case of integrating a 2 × 2 MMI coupler with the Mach–Zehnder modulator (MZM) of Ti:LN waveguides by replacing the waveguide Y-branch with the MMI coupler. Two complementary quadrature components are easily obtained simultaneously in two outputs. The 90-degree optical phase bias condition is theoretically satisfied without phase bias control.

Several studies on MMI in Ti:LN waveguides have been reported [8–10]. However, an MMI device structure having input–output waveguide ports has not yet been experimentally evaluated using Ti:LN waveguides to the authors' knowledge. We have shown the potential of MMI couplers of Ti:LN in a previous elementary experiment [11]. In the present work, MMI optical couplers consisting of Ti:LN waveguides were analyzed by the beam propagation method (BPM). Based on the results, we designed and fabricated a 2 × 2 MMI coupler and evaluated its properties. We also considered the electrical control of the device properties by forming electrodes on the MMI waveguide and experimentally evaluated the tuning of power splitting ratios of the coupler.

* Corresponding author.
E-mail address: enokihara@eng.u-hyogo.ac.jp (A. Enokihara).

https://doi.org/10.1016/j.optcom.2021.127325
Received 19 April 2021; Received in revised form 20 July 2021; Accepted 25 July 2021
Available online 8 August 2021

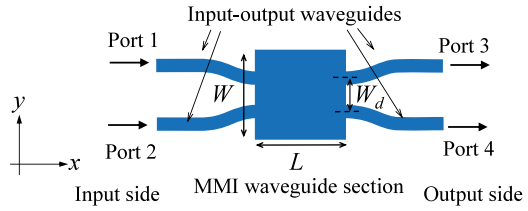

Fig. 1. Structure of 2 × 2 optical MMI coupler.

2. Analysis of MMI coupler of Ti:LN waveguide

2.1. Structure of MMI coupler

The structure of a symmetric 2 × 2 optical coupler based on MMI is shown in Fig. 1. The plane configuration is line-symmetric with the x-axis and the y-axis. Four input–output (IO) waveguides with single-mode propagation are connected to the MMI waveguide section of width W and length L. W_d is the distance between the connection positions of the IO waveguides at each end of the MMI waveguide. The incident light from one IO waveguide at the input side excites several propagation modes in the MMI waveguide section, which interfere with each other to form an image at the output end of the MMI waveguide. The propagation distance where a $\pi/2$ phase difference is induced between the two lowest-order modes in the MMI waveguide section is defined as the $\pi/2$ coupling length L_c. This corresponds to half the beat length of those two modes. When $L = L_c$ and the IO waveguides are connected at adequate positions, the field of input light from port 1 is theoretically reproduced at the end of the MMI waveguide section with the same amplitude and 90-degree phase difference for ports 3 and 4 by self-imaging [12]. Thereby, the waveguide circuit in Fig. 1 can operate as a 3 dB optical coupler. Representing the effective refractive indices of the fundamental mode and the next higher order mode as N_0 and N_1, respectively, the L_c is presented by

$$L_c = \frac{\lambda_0}{4(N_0 - N_1)}, \tag{1}$$

where λ_0 is the wavelength of light in free space. The $\pi/2$ coupling length obtained from the two lowest-order modes is approximately valid as the length of the MMI waveguide for the 3 dB coupler. Therefore, we considered the structure of the MMI optical coupler with reference to this coupling length.

2.2. Refractive index profile of Ti-diffused $LiNbO_3$ waveguide

We analyzed optical multimode waveguides of Ti:LN to determine whether they are applicable for MMI couplers. The refractive indices of Ti:LN waveguides gradually change across the cross section. Here we define the width of a Ti:LN waveguide as that of the line pattern of the Ti film prepared on the $LiNbO_3$ substrate before the diffusion, as shown in Fig. 2. The transverse profile of Ti ion concentration C by diffusion of the Ti film can be approximately presented by using the Gauss and error functions as [8]

$$C = \frac{\tau}{2\sqrt{\pi D_z t}} \exp\left(-\frac{z^2}{4D_z t}\right)\left[\mathrm{erf}\left(\frac{\frac{W}{2} - y}{2\sqrt{D_y t}}\right) + \mathrm{erf}\left(\frac{\frac{W}{2} + y}{2\sqrt{D_y t}}\right)\right], \tag{2}$$

where τ and t are the thickness of the Ti film and the diffusion time, respectively, and D_y and D_z are the surface and bulk diffusion constants, respectively, which are functions of the diffusion temperature T [°C]. Here we use the linear approximation for z-cut $LiNbO_3$ as $D_z = 7.971 \times 10^{-3}T - 7.578$ and $D_y = 2.057 \times 10^{-3}T - 1.656$ [8,13], where the unit of these constants is $\mu m^2/h$. The index change Δn_e for the extraordinary waves of $\lambda_0 = 1.55$ μm in a z-cut $LiNbO_3$ substrate can be presented as [14]

$$\Delta n_e = \left(\frac{\sqrt{\pi}C}{2}\right)^{0.81}\left[0.1293 + \frac{4.558\tau}{\sqrt{D_z t}}\mathrm{erf}\left(\frac{W}{4\sqrt{D_y t}}\right)\right]. \tag{3}$$

Using these equations, the change ratio of the refractive index $\Delta n_e/n_e$, where n_e is the extraordinary refractive index of $LiNbO_3$, was calculated. An example of the transverse profile of $\Delta n_e/n_e$ in the MMI waveguide section of $W = 50$ μm is shown in Fig. 3. The calculation conditions were determined based on our conditions for waveguide formation: $\tau = 85$ nm, $T = 990$ °C, and $t = 7.8$ h. We considered the propagation of the transverse magnetic (TM) modes, which have vertical electric fields.

2.3. $\pi/2$ coupling length of MMI waveguide

Next, the $\pi/2$ coupling length L_c was calculated for MMI waveguides with index profiles as determined by the equations in the previous section. The finite element beam propagation method (FE-BPM) [15] was used to calculate the effective refractive indices, N_0 and N_1, of the two lowest-order modes in the MMI waveguide. Fig. 4 shows L_c as a function of W. The waveguide formation conditions are the same as those in Fig. 3. It is found that L_c decreases as W decreases. With regard to the device size, a smaller W is preferable. However, it is known that the distance, W_d, between the two IO waveguides should be one third of the width, $W/3$, to realize a 3 dB coupler with a $\pi/2$ coupling length [12]. If W_d is too small, optical waves may be undesirably coupled between the two IO waveguides of the same side. When $W = 50$ μm, $W_d = W/3 = 16.7$ μm. This distance may be the minimum to avoid undesirable coupling for the 1.55 μm wavelength band. Therefore, we consider MMI couplers $W = 50$ μm, 60 μm, and 70 μm in the next section.

2.4. Optical properties of MMI coupler

We analyzed the optical properties of MMI couplers at $\lambda_0 = 1.55$ μm by the beam propagation method (BPM) for the cases of $W = 50$ μm, 60 μm, and 70 μm. The width of the IO waveguides was set to 7 μm for single-mode propagation, and W_d was set to $W/3$. Fig. 5 shows calculation results of optical power transmittances from port 1 to ports 3 and 4, normalized by the total transmittance, when an optical wave is incident at port 1. The insertion losses and the phase difference of the output light waves between ports 3 and 4 are also presented in the figures.

The power splitting ratios changed with L. At around $L = 2.2$ mm, 3.2 mm, and 4.3 mm, the incident light power is equally divided and the insertion losses are almost minimum for $W = 50$ μm, 60 μm, and 70 μm, respectively. The phase differences between the two outputs are also about 90 degrees at the L in all cases. We also calculated the wavelength dependence of the transmittance in the three cases by BPM analysis and found that there was no marked difference between the three cases. Therefore, we adopt an MMI waveguide of $W = 50$ μm, the smallest of the three cases, for miniaturization of the optical circuit structure. The length of 2.2 mm is roughly close to that of conventional Y-junctions of single-mode waveguides so that a 2 × 2 MMI optical coupler of $W = 50$ μm can be replaced with a conventional 1 × 2 Y-junction with regard to size.

We calculated the electric field distribution for $W = 50$ μm and $L = 2.2$ mm when light waves were incident at port 1, as shown in Fig. 6. Self-imaging caused by multimode interference is observed to reproduce the field at two positions corresponding to the two ports of the output side. It could be confirmed that the optical properties of the couplers in Fig. 5 were based on multimode interference in the Ti:LN waveguide.

3. Fabrication and measurement of MMI coupler

We fabricated an MMI coupler using Ti:LN waveguides and experimentally evaluated its optical properties. The waveguide pattern of the MMI coupler is shown in Fig. 7. Single-mode IO waveguides of 7 μm width were connected at both sides of the MMI waveguide section

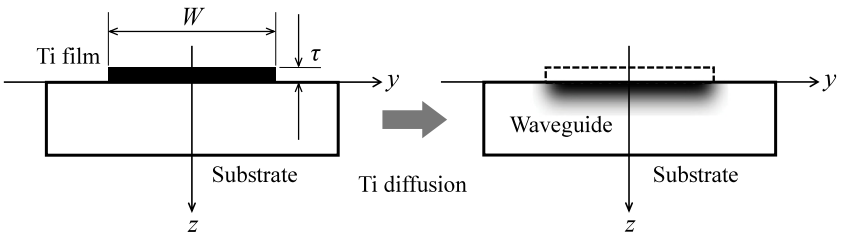

Fig. 2. Ti diffusion for an optical waveguide.

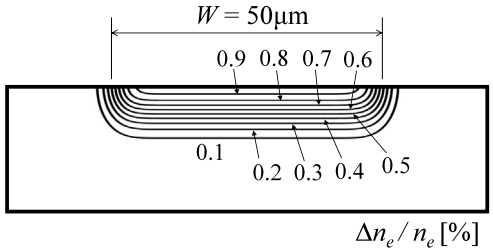

Fig. 3. Transverse profile of the change ratio of the refractive index by Ti diffusion for extraordinary waves in $LiNbO_3$.

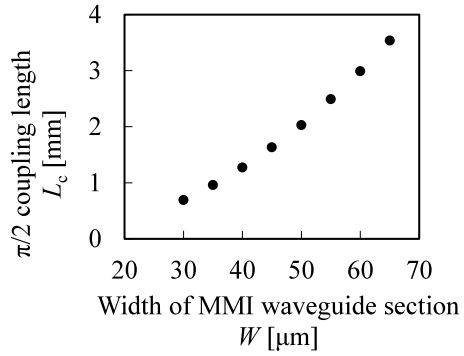

Fig. 4. $\pi/2$ coupling length L_c of the MMI waveguide as a function of waveguide width W.

of 50 μm width. The distance between the IO waveguides gradually increases to 50 μm by a sinusoidal curve, as shown in Fig. 7, for the convenience in coupling with optical fibers at the end faces of the substrate. The substrate was a 0.5 mm thick z-cut $LiNbO_3$ crystal. The optical waveguides were formed on the surface of the substrate by thermal in-diffusion of 85 nm thick Ti film patterns at 990 °C for 7.8 h in an oxygen atmosphere. MMI couplers of several lengths L, from 1.7 mm to 3 mm, of the MMI waveguide section were arranged on a single substrate.

First, to observe the transverse distribution of the optical electric field in the MMI waveguide, the MMI section was cut to expose the cross section at the end of the substrate. Near-field images of the end face were then observed by an infrared camera, as shown in Fig. 8. A laser source of 1.565 μm wavelength was used and the TM polarization mode was excited. Fig. 9 shows near-field images for several MMI waveguide lengths. The field gradually spreads over the MMI waveguide and concentrates at locations connected with the IO waveguides. Based on the figure, an efficient power split of the incident light is expected for the MMI.

We measured optical power transmittances from port 1 to ports 3 and 4 of the fabricated MMI couplers using a 1.565 μm laser source. Fig. 10 shows the optical power splitting ratio, which is the power transmittance to each port normalized by the sum of the power transmittances to both ports as a function of L. The insertion losses were normalized with that of a reference waveguide, which is a straight

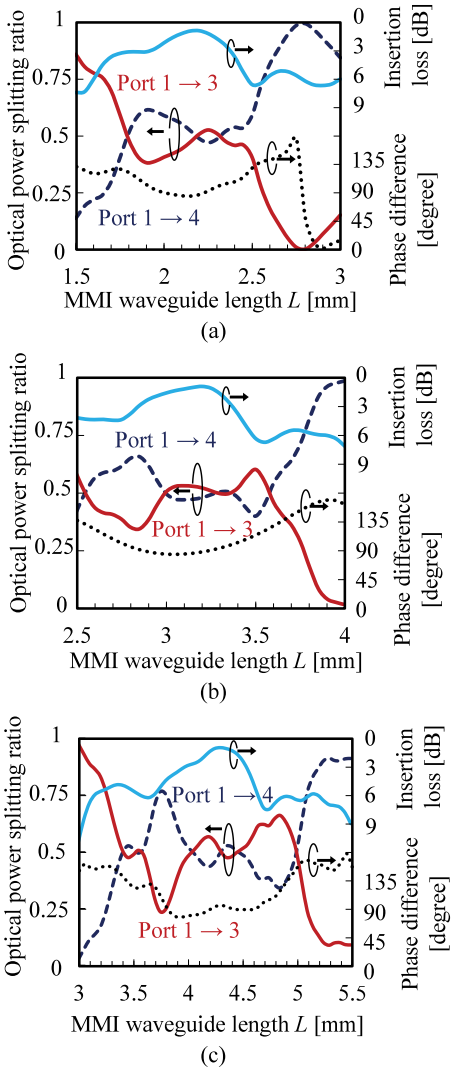

Fig. 5. Calculation results of optical properties of MMI couplers. (a) W = 50 μm, (b) W = 60 μm, and (c) W = 70 μm.

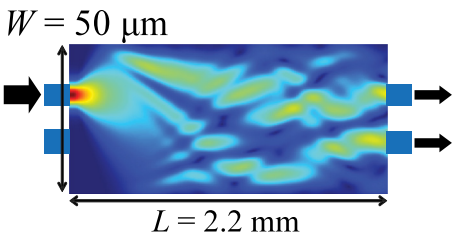

Fig. 6. Plane view of the electric field distribution calculated in the MMI waveguide section.

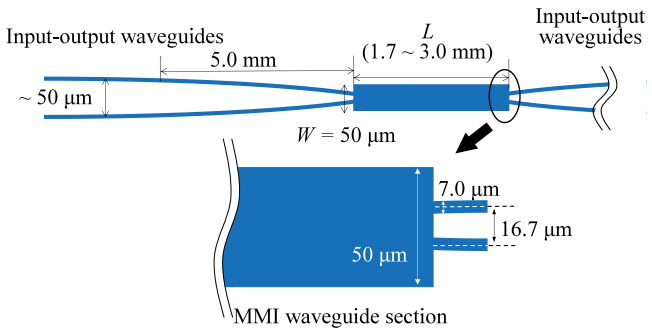

Fig. 7. Waveguide pattern of a 2 × 2 MMI coupler.

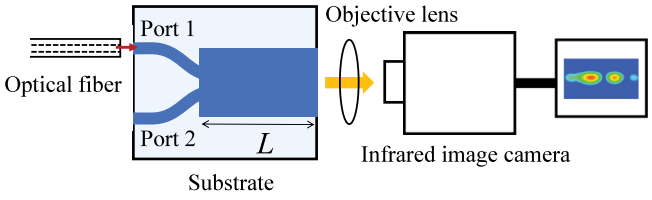

Fig. 8. Measurement setup for observing the transverse distributions of the optical electric fields in an MMI waveguide.

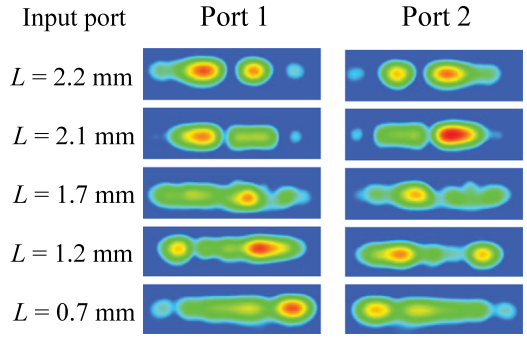

Fig. 9. Near-field images at the end face of the substrate.

single-mode waveguide formed on the same substrate, to remove the induced losses except for at the coupler section. From this figure, the optical power splitting ratio was 0.53:0.47 (0.52 dB power deviation) at $L = 2.12$ mm, which was the closest to being symmetric. There may have been another length close to 2.12 mm that would give a splitting ratio closer to equal splitting, but we fabricated a limited number of lengths. In the calculation of the previous section, the power splitting ratio was minimum at $L = 2.2$ mm, as shown in Fig. 5(a). This difference in the calculated and measured MMI section lengths can be attributed to the refractive index distribution of Eq. (3) not being perfectly matched to the actual situation in the experiment.

The measured insertion losses of the MMI coupler section were less than 1.5 dB between $L = 2.1$ and 2.2 mm and 1.15 dB at $L = 2.12$ mm. The loss when the power splitting ratio was closest to equal splitting was 0.80 dB in the BPM analysis, as shown in Fig. 5(a), and was 0.35 dB lower than that of the experiment. This difference may be partly due to the fact that the analysis does not consider any material losses induced in the MMI waveguide. Although the phase difference between two light outputs of the MMI coupler could not be measured, it can be evaluated that the MMI coupler of length L around 2.12 mm was operating as a 3 dB optical coupler.

4. Tuning of optical power splitting ratio

MMI devices of Ti:LN waveguides are expected to exhibit the ability to tune the device properties by EO effects. The power splitting ratios

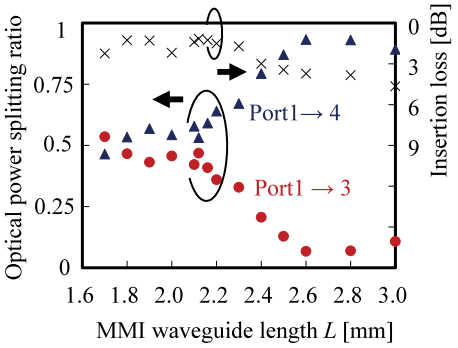

Fig. 10. Measurement results of optical properties of the MMI coupler.

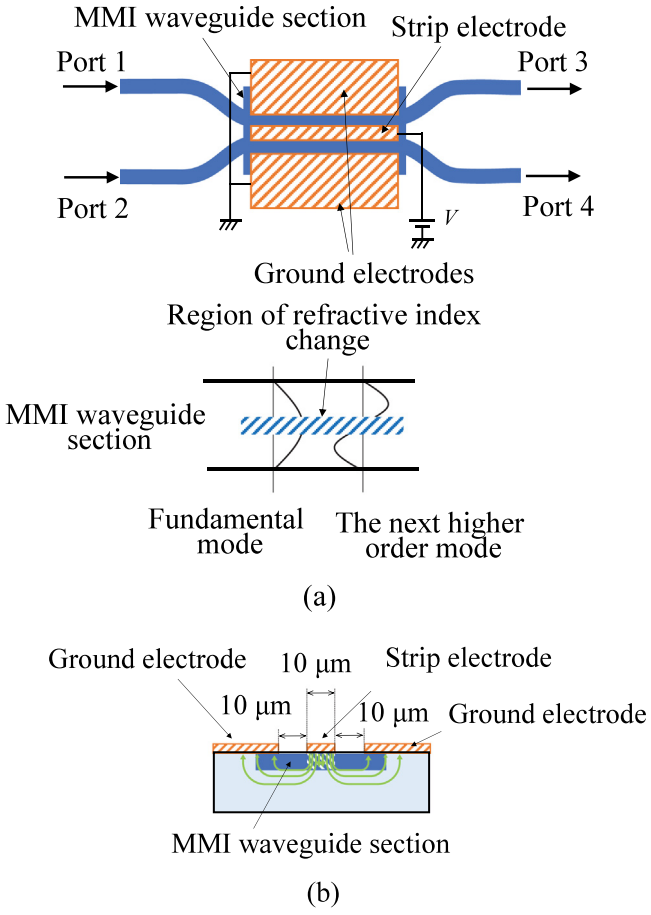

Fig. 11. MMI coupler with electrodes for electrical tuning of power splitting ratios. (a) Plane view, (b) cross-sectional view.

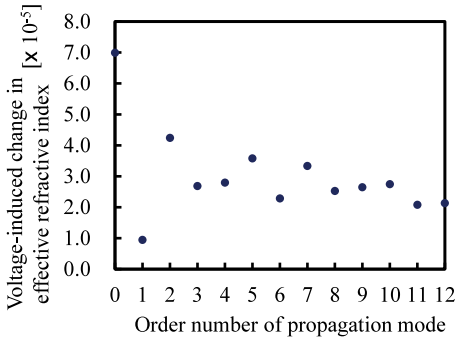

Fig. 12. Change in effective refractive index of the propagation modes in an MMI waveguide of 50 μm width when applying ±10 V to the strip electrode.

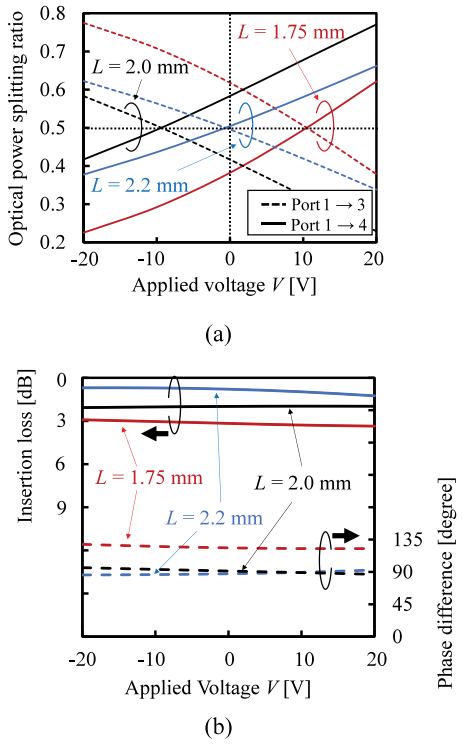

Fig. 13. Optical properties of MMI couplers calculated as a function of applied voltage. (a) Optical power splitting ratios and (b) insertion losses and phase differences between two light outputs.

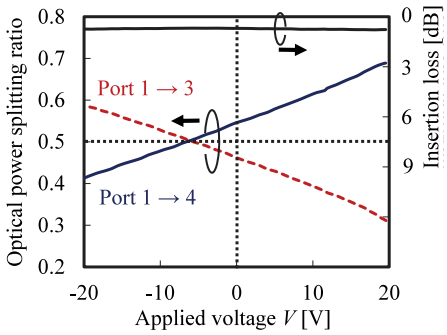

Fig. 14. Measurement results of optical power transmittances as a function of applied voltage.

can be changed by inducing a partial change in the refractive index of the MMI waveguide. It has been reported that the power splitting ratios can be tuned by modifying the refractive index around selected spots where self-images are formed within the MMI waveguides [16,17]. Here, we consider the electrical control of the difference between the effective refractive indices N_0 and N_1 in Eq. (1) to change the coupling length L_c. Thereby the power splitting ratios are expected to be tuned by smaller changes of refractive index compared to the previous studies detailed above. Another tuning method based on the thermo-optical effect has also been reported for MMI couplers using silicon waveguides [18]. Although this method is applicable to most materials including Si and SiO_2, the tuning by the EO effect is advantageous in terms of response speed and the accuracy of the adjustment.

Fig. 11 shows an MMI coupler with electrodes designed for tuning the power splitting ratios by the EO effect. A strip electrode of 10 μm width is located in the center of the width direction of the MMI waveguide on a z-cut LN substrate. Ground electrodes are arranged at both sides of the strip electrode with a spacing of 10 μm. A vertical electric field is generated immediately below the strip electrode by applying a voltage as shown in Fig. 11(b). The extraordinary index of this area is effectively changed by the EO effect. Thereby, the propagation modes of the even symmetric field, such as the fundamental mode, are more greatly affected regarding their effective refractive index than those of the odd symmetric field, such as the next higher order mode, as shown in Fig. 11(a). The influence of the electric field generated under the ground electrodes on the power splitting ratio was small enough that the electric fields of the ground electrodes could be ignored in this analysis.

Fig. 12 shows calculations of the voltage-induced change in the effective refractive index of the TM propagation modes in the MMI waveguide when applying ±10 V to the strip electrode. The calculations were performed using EO coefficients of $LiNbO_3$ under the assumption that the induced fields were located only immediately under the strip electrode. It is found that there is a particularly large difference in the index change between the two lowest-order modes. Therefore, it is expected that L_c is effectively changed according to Eq. (1) and that the power splitting ratio can be controlled by the applied voltage. The optical properties were calculated by the BPM with the same conditions as previously. Fig. 13(a) shows the optical power splitting ratios of the MMI coupler for several MMI waveguide lengths L for an optical wave incident at port 1. The insertion losses and phase difference of the output light waves between ports 3 and 4 are presented in Fig. 13(b). It is found that the power splitting ratios are changed almost in proportion to the voltage and that all the curves of the splitting ratios pass through points of the equal splitting of 0.5. Focusing on the case of $L = 2.0$ mm in Fig. 13(a), the power splitting ratio of about 0.6:0.4 at $V = 0$, which is about 1.8 dB deviation from equal split, can be adjusted to the equal split state by applying a voltage of around −10 V. The insertion losses and the phase differences are almost unchanged by applying the voltage, as shown in Fig. 13(b).

In order to experimentally confirm this tuning feature, an MMI coupler with electrodes was fabricated. The fabrication conditions of the waveguides were the same as previously. The MMI waveguide length was fixed at 1.9 mm, which is slightly different from the length for the equal split. The electrodes consist of a gold film of 1 μm thickness patterned by the photolithographic method. An SiO_2 buffer layer of 670 nm thickness was formed between the substrate and the electrodes to avoid light power losses. Fig. 14 shows the measurements of the optical power splitting ratio as a function of applied voltage. The insertion losses of the coupler section are also indicated. It is seen that the power splitting ratio changed almost in proportion to the voltage in the same way as the calculation and that the 1.0 dB power deviation (0.56:0.44) in the power splitting from an equal split at $V = 0$ could be adjusted to zero by applying a voltage of −6.1 V. The insertion losses were almost unchanged by the tuning. It is shown that the power splitting ratio was effectively controlled by applying a voltage and that a perfectly symmetric power splitting could be also obtained.

5. Conclusion

We designed and fabricated 2 × 2 MMI optical couplers using Ti:LN waveguides. The MMI couplers were analyzed with BPM taking account of the refractive index distributions based on Ti diffusion. The couplers were fabricated and their optical properties were experimentally measured. An optical power splitting ratio of 53:47 (0.52 dB power deviation from symmetry) and less than 1.5 dB insertion loss were observed with a coupler consisting of an MMI waveguide 50 μm wide and 2.12 mm long. We also considered electrical tuning of the optical power splitting ratio by applying a voltage to electrodes directly formed on the MMI waveguide. In the experiment, the power splitting ratio of 0.56:0.44 without applying a voltage could be adjusted to an equal splitting by a voltage of −6.1 V. It was shown that an optical coupler with a perfectly equal split could be obtained by electrical tuning using

the EO effect of $LiNbO_3$. Based on these results, optical MMI couplers consisting of Ti:LN waveguides can be expected for application to EO devices, such as high-speed optical modulators, as important optical circuit elements.

Declaration of competing interest

The authors declare that they have no known competing financial interests or personal relationships that could have appeared to influence the work reported in this paper.

Acknowledgments

The authors thank Prof. Tetsuya Kawanishi of Waseda University and Dr. Atsushi Kanno of National Institute of Information and Communications Technology for their valuable cooperation in this work. This work is supported by KAKENHI Grant number 20K04601 of JSPS, Japan.

References

[1] L.B. Soldano, E.C.M. Pennings, Optical multi-mode interference devices based on self-imaging: Principles and applications, J. Lightwave Technol. 13 (4) (1995) 615–627.

[2] S.H. Jeong, K. Morito, Novel optical 90° hybrid consisting of a paired interference based 2 × 4 MMI coupler, a phase shifter and a 2 × 2 MMI coupler, J. Lightwave Technol. 28 (9) (2010) 1323–1331.

[3] S. Pathak, M. Vanslembrouck, P. Dumon, D. Van Thourhout, W. Bogaerts, Optimized silicon AWG with flattened spectral response using an MMI aperture, J. Lightwave Technol. 31 (1) (2013) 87–93.

[4] A. Irace, G. Breglio, All-silicon optical temperature sensor based on multi-mode interference, Opt. Express 11 (22) (2003) 2807–2812.

[5] R. Cheng, D. Zhang, J. Wang, C. Wang, F.i Gao, X. Sun, Z. Shi, Z. Cui, C. Chen, Fluorinated photopolymer cascaded MMI-based integrated optical waveguide switching matrix with encoding functions, Opt. Express 27 (9) (2019) 12883–12898.

[6] Y. Wei, G. Li, Y. Hao, Y. Li, J. Yang, M. Wang, X. Jiang, Long-wave infrared 1 × 2 MMI based on air-gap beneath silicon rib waveguides, Opt. Express 19 (17) (2011) 15803–15809.

[7] Z. Sheng, Z. Wang, C. Qiu, L. Li, A. Pang, A. Wu, X. Wang, S. Zou, F. Gan, A compact and low-loss MMI coupler fabricated with CMOS technology, IEEE Photonics J. 4 (6) (2012) 2272–2277.

[8] L.P. Shen, H. Wang, C. Xu, W.P. Huang, Numerical analysis of multimode interference effect in Ti:$LiNbO_3$ waveguides, in: Proceedings of SPIE, vol. 5970, 59700W, Photonics North 2005, Toront Canada, Oct., 2005.

[9] Y. Yao, W. Wang, B. Zhang, Designing MMI structured beam-splitter in $LiNbO_3$ crystal based on a combination of ion implantation and femtosecond laser ablation, Opt. Express 26 (15) (2018) 19648–19656.

[10] Y.L. Lee, T.J. Eom, W. Shin, B.A. Yu, D.K. Ko, W.K. Kim, H.Y. Lee, Characteristics of a multi-mode interference device based on Ti:$LiNbO_3$ channel waveguide, Opt. Express 17 (13) (2009) 10718–10724.

[11] A. Hirai, T. Sato, T. Kawai, A. Enokihara, S. Nakajima, N. Yamamoto, Design and fabrication of MMI optical coupler using Ti-diffused Lithium Niobate waveguides, in: 2020 International Topical Meeting on Microwave Photonics, MWP, Nov., 2020, pp. 173–176.

[12] M. Bachmann, P.A. Besse, H. Melchior, Overlapping-image multimode interference couplers with a reduced number of self-images for uniform and nonuniform power splitting, Appl. Opt. 34 (30) (1995) 6898–6910.

[13] M. Fukuma, J. Noda, Optical properties of titanium-diffused $LiNbO_3$ strip waveguides and their coupling-to-a-fiber characteristics, Appl. Opt. 19 (4) (1980) 591–597.

[14] S. Fouchet, A. Carenco, C. Daguet, R. Guglielmi, L. Riviere, Wavelength dispersion of Ti induced refractive index change in $LiNbO_3$ as a function of diffusion parameters, J. Lightwave Technol. 5 (5) (1987) 700–708.

[15] Y. Tsuji, M. Koshiba, Finite element beam propagation method with perfectly matched layer boundary conditions for three-dimensional optical waveguides, Int. J. Numer. Modelling, Electron. Netw. Devices Fields 13 (2–3) (2000) 115–126.

[16] J. Leuthold, C.H. Joyner, Multimode interference couplers with tunable power splitting ratios, J. Lightwave Technol. 19 (5) (2001) 700–707.

[17] D.A. May-Arrioja, P. LiKamWa, C. Velásquez-Ordóñez, J.J. Sánchez-Mondragón, Tunable multimode interference coupler, Electron. Lett. 43 (13) (2007) 714–716.

[18] Á. Rosa, A. Gutiérrez, A. Brimont, A. Griol, P. Sanchisásquez-Ordóñez, J.J. Sánchez-Mondragón, High performace silicon 2 × 2 optical switch based on a thermo-optically tunable multimode interference coupler and efficient electrodes, Opt. Express 24 (1) (2016) 191–198.